Hindawi
Advances in Civil Engineering
Volume 2021, Article ID 5574934, 13 pages
https://doi.org/10.1155/2021/5574934

Research Article

Analysis of Vertical Load Transfer Mechanism of Assembled Lattice Diaphragm Wall in Collapsible Loess Area

Mingtan Xia,[1] Xudong Zhang,[1] Gengshe Yang,[2] Liu Hui ,[2] and Wanjun Ye[2]

[1]*China Railway 11 Burea Group Co., Ltd., Wuhan, China*
[2]*College of Architecture and Civil Engineering, Xi'an University of Science and Technology, Xi'an, China*

Correspondence should be addressed to Liu Hui; 67646930@qq.com

Received 7 January 2021; Accepted 23 June 2021; Published 8 July 2021

Academic Editor: Zhang Dongmei

Based on analysis of the formation mechanism and characteristics of the negative friction in collapsible loess areas, this study investigates the load transfer law of a wall-soil system under a vertical load, establishes the vertical bearing model of a lattice diaphragm wall, and analyzes the vertical bearing capacity of an assembled latticed diaphragm wall (ALDW) in a loess area. The factors influencing the vertical bearing characteristics of the ALDW in a loess area are analyzed. The vertical bearing mechanism of the lattice diaphragm wall in the loess area is investigated. The failure modes of the ALDW in the loess area are mainly shear failure of the soil around the wall and failure of the wall-soil interface. In the generation and development of negative friction, there is always a point where the relative displacement of the wall-soil interface is zero at a certain depth below the ground; at this point, the wall and soil are relative to each other. The collapsibility of loess, settlement of the wall and surrounding soil, and rate and method of immersion are the factors affecting the lattice diaphragm wall. The conclusions of this study provide a reference for the design and construction of ALDWs in loess areas.

1. Introduction

Through many years of urban construction practice, relatively mature enclosure structure designs have been developed for different foundation pit conditions. The commonly used retaining structures include diaphragm walls, bored piles, steel sheet piles, soil mix wall (SMW) methods, cement-soil mixing piles, and composite soil nail walls. With the development of modern construction technology, diaphragm walls can serve the functions of acting as a gravity retaining wall, bearing the vertical load of the structure, and providing waterproofing.

The assembled lattice diaphragm wall (ALDW) retaining structure is a new type of retaining structure that has been applied in foundation pit engineering in recent years [1, 2]. Because of its unique geometric structure, it has many advantages in deformation control and sustainable development and can meet the requirements of shortening the construction period and reducing land occupation. As a result, ALDWs have become a new structural form for public foundation pit support.

In the excavation stage of a foundation pit, the lattice diaphragm wall is used as an enclosure structure and seepage control structure. After excavation of the foundation pit, it can begin to function as the regular use stage. Because the lattice diaphragm wall has very high strength and individual vertical bearing capacity, it can directly bear the vertical load of the upper structure as part of the main structure or as the main structure itself. The lattice diaphragm wall can play a role in the enclosure structure during the construction period, while it can also play the role of vertical support in the use stage. Fully utilizing the lattice diaphragm wall structure can effectively reduce project costs. ALDWs have played an essential role in urban construction in Xi'an, particularly for subway construction.

Many scholars [3–7] have studied the bearing characteristics of diaphragm walls in different strata. Previous research on lattice wall retaining structures has mainly employed field monitoring, centrifugal model tests, and numerical simulations. In terms of field monitoring, Mei [8] determined that the horizontal deformation law of a lattice

wall retaining structure is similar to that of a gravity retaining structure based on deformation data measured for a dock foundation pit. The field monitoring data reported by Liang et al. [9] showed that the ratio of the horizontal displacement of the lattice wall to the excavation depth of the foundation pit was between 0.15% and 0.50%, and the horizontal displacement of the lattice wall was significantly lower than that of a tension anchor diaphragm wall. In terms of centrifugal model tests, Zuo et al. [10] noted that the variation in the Earth pressure between the front and back walls was not obvious based on centrifugal model tests of a lattice wall in sand. The centrifugal model test results for a lattice wall in soft soil reported by Zhou et al. [11] showed that the Earth pressure in the passive zone was greater than the Rankine passive Earth pressure, whereas the Earth pressure in the active zone was greater than the Rankine active Earth pressure but less than the static Earth pressure. Chen et al. [12] demonstrated that the bending moment, deformation, and Earth pressure of a lattice wall in clay were greater than those in sand. In terms of numerical simulations, Hou [13] studied the stress deformation characteristics and strata displacement law of a lattice wall during foundation pit excavation based on the finite element method and carried out extensive parameter analyses. The ideal elastic-plastic Coulomb friction model was used to describe the tangential contact characteristics between the wall and soil.

Masuda [14] collected data measured for 52 foundation pits in different areas of Japan having a diaphragm wall as the enclosure. The analysis results showed that the maximum lateral displacement of the diaphragm wall in sandy soil was approximately 0.05%–0.5% of the excavation depth, and the maximum lateral displacement in the clay layer was generally less than 0.5% of the excavation depth. Thus, these measures can effectively reduce displacement. Carder [15] collected data for the deformation of pits enclosed by cast-in-place piles and continuous walls in Britain under hard clay conditions. The results showed that the maximum lateral displacement limits of the enclosure structures were 0.125% H, 0.2% H, and 0.4% H at high, medium, and low stiffness, respectively. Yoo [16] analyzed the measured data for foundation pit projects in Seoul and other regions of Korea. It was found that the maximum lateral displacement of the diaphragm wall foundation pit was 0.05% H, while that of other supports was 0.13%–0.15% H, and the maximum lateral displacement of the anchor support was slightly smaller than that of the inner support. Moormann [17] collected a large amount of deformation data for foundation pits worldwide using methods similar to those of Long [18]. The deformation laws of small support structures under each soil condition were analyzed, and the influences of the type of enclosure structure and support on the deformation were discussed. Zuo et al. [10] used centrifuge tests to investigate the mechanical properties and deformation characteristics of the foundation of a grille diaphragm wall in sandy soil. To investigate the applicability of the lattice-shaped diaphragm wall (LSDW) as a bridge foundation in soft soil, Wu et al. [1] considered three models (a pile group, LSDW with a single chamber, and LSDW with two chambers) having similar material quantities using small-scale model tests and numerical analyses based on FLAC3D. The soil arching effect of the LSDWs was investigated based on PFC2D, and special attention was given to the influencing factors [19]. Wu et al. [20] carried out comparative model tests on three types of foundations (group pile, single room diaphragm wall, and two-room grid diaphragm wall) with similar material quantities. The results showed that, in soft soil, using a diaphragm wall foundation instead of a group pile could improve the bearing capacity of the foundation and reduce settlement.

The current research mainly focuses on foundations with a single-chamber diaphragm wall [21, 22], while research on foundations comprising ALDWs is still in its infancy. Cheng [23] introduced the mechanism and application prospects of using a grid diaphragm wall to provide antiliquefaction capability under earthquakes. Hou [24, 25] studied the vertical bearing mechanism of a lattice diaphragm wall based on in situ static load tests and three-dimensional finite element analysis. Xie et al. [26] presented lattice-shaped diaphragm wall as a new method of foundation improvement for high embankment culverts on soft foundation; high strength exchanging-fill materials are adopted to partially replace the foundation soil. Wu et al. [27] conducted a numerical study to compare the static and seismic responses of LSDWs and pile groups having similar material quantities in soft soil.

As a new type of bridge foundation, the ALDW is highly applicable in practical engineering; however, theoretical research on its vertical bearing capacity is insufficient, especially in areas of collapsible loess. Xi'an is a typical collapsible loess area; it has high strength under natural humidity, and its structural damage and strength decrease significantly after being wetted. The soil skeleton structure is destabilized, and collapsible deformation occurs under the action of the soil self-weight or overlying load. The collapsible deformation of the soil causes relative displacement of the wall and soil, which leads to negative friction of the pile side, thus increasing the wall settlement and decreasing the bearing capacity. At present, research on the vertical bearing characteristics of lattice diaphragm walls in loess areas has not been carried out. There is thus an insufficient theoretical basis for this new type of bearing structure, especially regarding its bearing mechanism, design, and vertical bearing capacity calculation method, which limits the practical applications of the project. Therefore, it is of practical engineering significance to analyze the load-bearing mechanism of ALDWs in loess areas.

2. Structure of the Lattice Diaphragm Wall

The total length of the Xi'an Metro Phase III line is 280.8 km, with 156 stations, which encounters many problems of foundation pit support. The excavation depth of these foundation pits is large. Due to the complex building environment around the city, the traditional prefabricated diaphragm wall cannot play a role when the foundation pit support system cannot set internal support. In addition, in the subway deep foundation pit excavation, the width of the

foundation pit is large; if the internal support is used, it must be used with columns; otherwise, its stability cannot be guaranteed, which undoubtedly limits the internal operation space of the foundation pit, which is extremely inconvenient for mechanized construction, and the ALDW can make up for the above shortcomings.

The ALDW is a lattice structure connected by a series of grooves on the diaphragm wall, as shown in Figure 1. The lattice diaphragm wall is composed of inner and outer longitudinal walls and transverse diaphragm walls. The lattice structure composed of inner and outer longitudinal walls and the undisturbed soil inside the diaphragm wall jointly form a semigravity structure. As the retaining structure of a foundation pit, the water and soil pressure outside the pit can be borne by the lattice diaphragm wall during the construction of the foundation pit. The lattice diaphragm wall is a semigravity self-supporting retaining structure. It has the advantages of a diaphragm wall, that is, high stiffness and excellent impermeability, which can better limit the deformation of the foundation pit and bear the vertical load.

The upper structure is loaded as a permanent structure. A T-shaped groove section is usually used at the intersection of the diaphragm wall and inner and outer longitudinal walls to improve the integrity of the lattice diaphragm wall. At present, the thickness of the groove section of the diaphragm wall is typically 50–120 cm, although the thickness can reach 320 cm. The soil depth is generally in the range of 10–50 m, although the maximum depth can reach 170 m.

The wall can be considered as an infinite elastic body. The external force is parallel to the cross section of the wall and remains constant along the length direction; therefore, it can be regarded as a plane strain problem.

3. Formation Mechanism and Negative Friction Characteristics of the Lattice Diaphragm Wall in a Collapsible Loess Area

3.1. Formation of Negative Friction Resistance. The problem of wall frictional resistance is essentially a contact problem caused by the interaction between the wall and soil. Because of the difference in material properties between the soil and wall, the relative displacement between the wall and soil is nonzero under vertical loading, which leads to the generation of wall side friction. When the wall moves downward relative to the soil under a vertical load, the soil produces upward shear stress, i.e., positive friction resistance, owing to the relationship between the action force and the reaction force. However, in a collapsible loess area, the collapsibility of the loess often causes the soil around the wall to move downward relative to the wall. This produces downward shear stress on the wall, i.e., negative friction. The distribution and variation of the negative frictional resistance are highly complex. The settlement, velocity, and stability of the soil around the walls and piles, the collapsibility of the loess, the immersion method, and the duration of immersion all have different effects on the negative frictional resistance.

3.2. Collapse Displacement Load Transfer Principle. For a wall whose bearing capacity is mainly borne by the interaction at the wall-soil interface, if the interaction between the walls is not considered, the settlement displacement between the soil elements far from the center of the wall will be synchronized after the foundation is immersed and collapsible. There is no collapsible load transfer; therefore, it is a noncollapsible load transfer range. Within a specified thickness range from the wall, the settlement displacement of the adjacent soil elements differs, which is within the scope of the collapsible load transfer.

As shown in Figure 2, the soil in a range x from the center of the wall is within the range of collapsible load transfer. After collapsing, the farthest element in the influence range, $ABCD$, sinks to the location of $A'B'C'D'$ under gravity. This generates a downward shear force on the adjacent element, $CDEF$. $ABCD$ transfers a load to $CDEF$ through the difference in collapsible displacement, and $CDEF$ sinks and deforms accordingly to state $C'D'E'F'$. In the elemental analysis with a width dr and thickness in this range, the transfer of the collapsible load is an energy transfer process. The displacement, SG, occurs under the action of gravity, G. The work of gravity, $SG{\cdot}G$, is a dynamic source of collapsibility. Under the shear force and action, $\tau\imath$, of adjacent elements on both sides, shear deformation and volume deformation of the element occur. In the plastic deformation part of the lossy collapsible energy, the residual collapsible potential is transmitted to the adjacent elements on one side of the wall through shear force (which is related to the bonding and particle friction). Thus, the collapsible potential decreases gradually as it approaches the wall, and the subsidence displacement of the soil element decreases, finally reaching the surface element of the wall, HH. The load is a negative friction, q. The collapsible load transfer process can be described as follows:

$$f \cdot S_f \propto [(G \cdot S_G)\colon \tau], \tag{1}$$

where S_f is the action range of the negative friction in the length direction of the wall. If the action distance of the negative friction along the wall is equal to the settlement displacement of the soil around the wall, the equation can be written as follows:

$$f \propto [G\colon \tau]. \tag{2}$$

Equation (2) shows that the collapse process is formally transformed from a physical force (gravity) to a surface force (negative friction).

The elastic modulus, E, and shear modulus, G, of the soil around the wall vary in the radial direction. The closer the collapse is to the wall, the more energy is dissipated by plastic deformation and the smaller the shear deformation will be under the same shear stress.

3.3. Calculation of the Negative Friction Resistance Based on the Load Transfer Method. In the wall with a depth of l, the upper soil will be displaced downward relative to the wall (the maximum, s, is at the surface), which produces negative

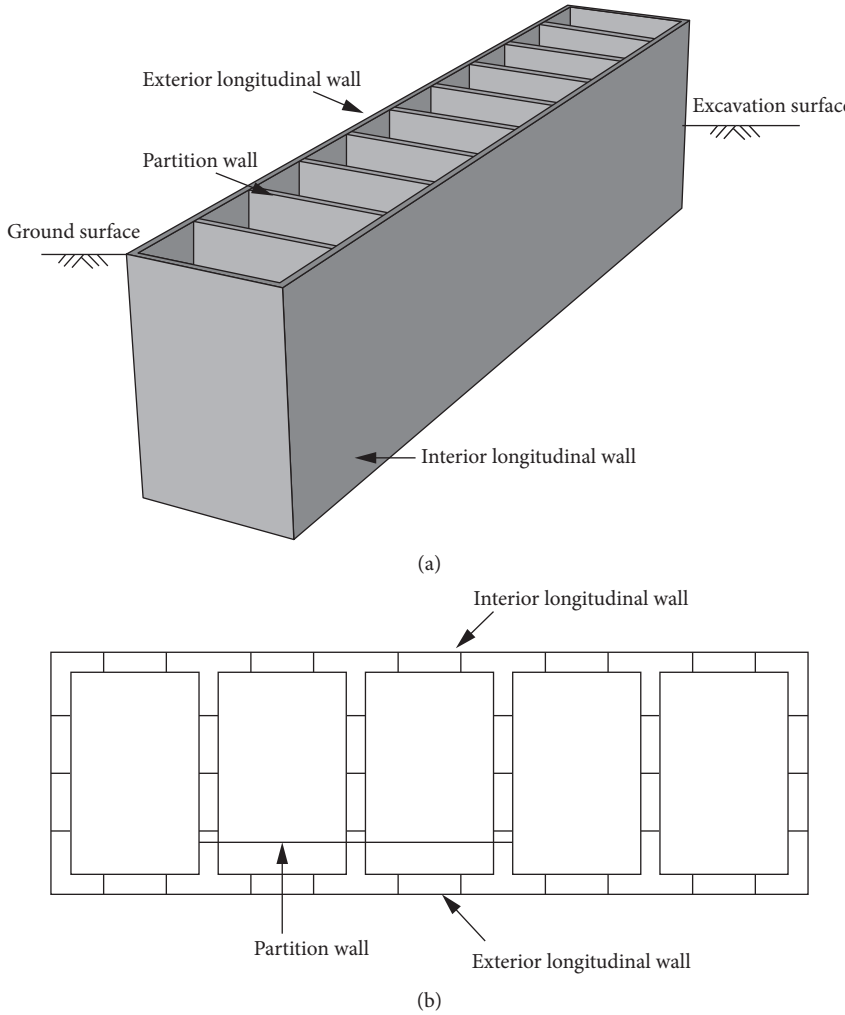

Figure 1: Structural sketch of the lattice diaphragm wall. (a) 3D view. (b) Top view.

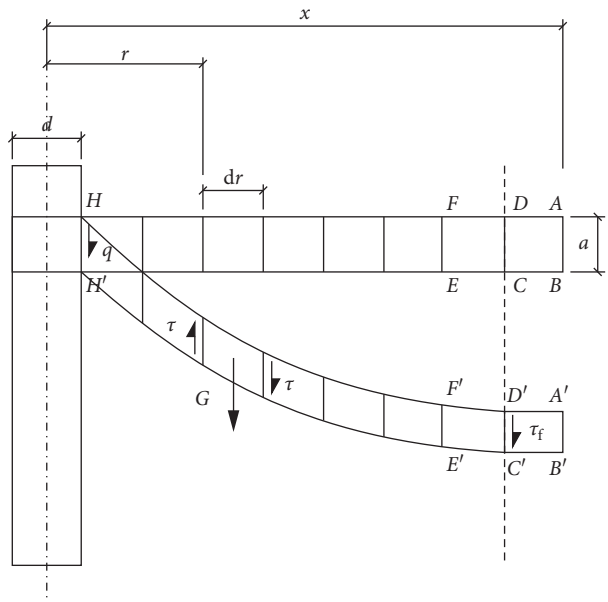

Figure 2: Principle of collapsible load transfer.

friction, q, and acts on the wall, causing the end of the wall to sink into the soil by δl; the end resistance, Qb, also plays a role. The soil near the end of the wall shows a positive friction, q', as shown in Figure 3(a). The contribution of the wall compressive deformation to the wall top displacement under negative friction is δ_f (including the total displacement, δ_0, of the wall top sinking through deformation). The movement of the soil relative to the wall is zero at vertical position ln; that is, the neutral point is located there. The displacement of the decomposed wall and the corresponding lateral resistance are shown in Figures 3(b) and 3(c).

It is assumed that the interface between the wall and soil is fully contacted, the diaphragm wall material is completely linearly elastic and is not destroyed before reaching the ultimate bearing capacity, and the mechanical action of the contact surface of the wall-soil element is a spring action model. The equilibrium equation can be obtained by considering the microelement dz at depth z as follows:

$$Uq\mathrm{d}z + N(z) + \mathrm{d}N(z) = N(z), \tag{3}$$

$$q = -\frac{1}{U}\frac{\mathrm{d}N(z)}{\mathrm{d}z}. \tag{4}$$

For elastic member element dz, $\mathrm{d}N(z) = EA(\mathrm{d}u(z)/\mathrm{d}z)$. Substituting this into equation (4) yields the following:

$$q = -\frac{1}{U}EA\frac{\mathrm{d}^2u(z)}{\mathrm{d}^2z}. \tag{5}$$

Equation (5) is the transfer differential equation for the negative frictional resistance, U is the circumference of the wall cross section, and $N(z)$ is the axial force of the wall at depth z.

The negative frictional resistance, q, is an irregular distribution along the wall and a function of the depth, z, defined as $q(z)$. The key to solving the equation is to determine the functional relationship between $q(z)$ and the relative displacement, $u(z)$. For this reason, many scholars have proposed $q(z)$–$z(u)$ distribution functions to improve the calculation of the negative frictional resistance, for example, Sato's double-folded line model and the linear elastic full-plastic model.

Negative frictional resistance has several unique characteristics, as described as follows.

3.3.1. Neutral Point. During the generation and development of negative frictional resistance, there always exists a point at a certain depth below the ground at which the relative displacement between the wall and soil is zero. The soil moves downward relative to the wall in the section above this point, and the wall is subjected to a negative frictional resistance. The wall moves downward relative to the soil in the section below this point, and the wall is subjected to positive friction. The inflection point of the wall frictional resistance is the neutral point under the action of resistance, as shown in Figure 4. The neutral point has three distinct characteristics: the relative displacement of the wall and soil at this point is zero, the friction resistance is zero, and the axial force is the maximum. The main factors affecting the location of the neutral point are the degree of immersion, collapsibility of the soil around the wall, stress history, stiffness of the bearing layer at the end of the wall, and length-to-diameter ratio of the wall.

3.3.2. Time Effect of the Negative Friction Resistance. Because the negative friction on the wall side involves settlement of the soil around the wall, its development process is affected by the completion time of the settlement. Analyses can be performed according to the neutral point and pull-down load.

(i) Time effect of the neutral point: the position of the neutral point constantly changes as the wall and soil settle. Because the settlement of the soil around the wall and the wall itself is time-dependent, the position of the neutral point also has a time dependency. Generally, the position of the neutral point moves downward with time; however, if the settlement of the soil is completed before the wall sinks, the neutral point will move upward. Finally, when the relative displacement of the wall and soil is stable, the position of the neutral point also tends to be stable.

(ii) Time effect of the pull-down load: the pull-down load refers to the downward force exerted on the wall by the soil around the wall as it moves downward relative to the wall, that is, the area integral of negative friction in the extended area of the wall. The pull-down load also has a time dependency. The pull-down load development can be divided into two stages according to the development speed of the negative friction. As shown in Figure 5, the process can be described in two parts: first, the negative friction develops rapidly with time, and the pull-down load also increases rapidly; then, as the negative friction approaches the limit value, it increases more gradually, and ultimately the negative friction increases to be a stable limit value.

4. Vertical Load Transfer Mechanism of the ALDW in a Loess Area

4.1. Vertical Bearing Capacity of the Lattice Diaphragm Wall in a Loess Area. Because of its complex structure, the vertical bearing mechanism of the ALDW is more complex than that of an ordinary diaphragm wall. Under a vertical load, the core soil, inner and outer longitudinal walls, and wall end soil of the diaphragm wall in a loess area bear the upper load together. Therefore, the vertical bearing capacity, Q_u, of the lattice diaphragm wall in a loess area is mainly composed of five parts: the side friction, Q_s, provided by the lateral soil; negative friction, Q_f, of the collapsible loess; side friction, Q_{si}, provided by the core soil; negative friction, Q_{fi}, of the collapsible loess; and end resistance, Q_p, of the lattice diaphragm wall. The vertical bearing capacity can be expressed as follows:

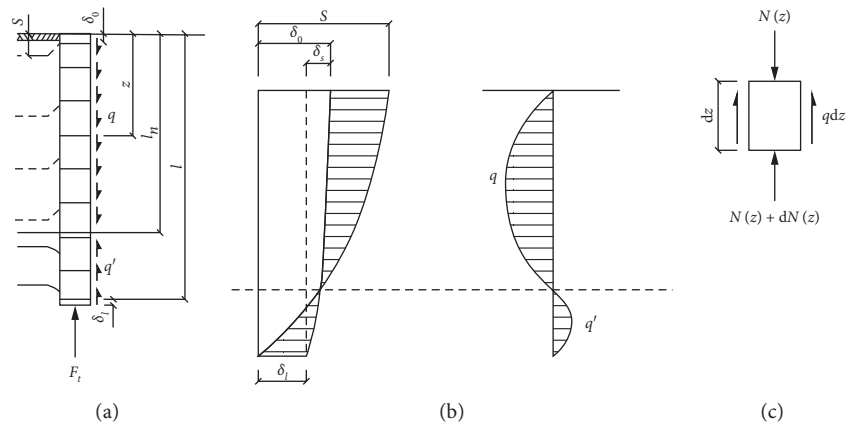

Figure 3: Schematic diagram of the calculation of negative friction in a lattice diaphragm wall located in a loess area.

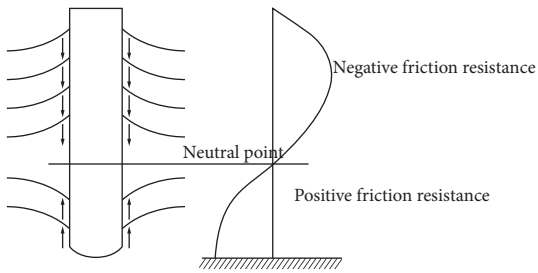

Figure 4: Neutral point diagram.

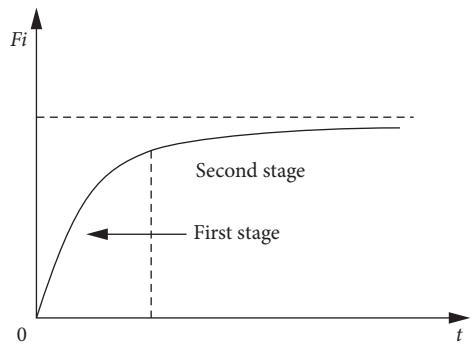

Figure 5: Two stages of pull-down load development.

$$Q_u = Q_s - Q_f + Q_{si} - Q_{fi} + Q_p. \tag{6}$$

Assuming that the distribution of the lateral friction, Q_s, provided by the soil outside the lattice diaphragm wall is similar to that of a pile foundation, the calculation equation for the lateral friction, Q_s, provided by the soil outside the lattice diaphragm wall refers to the equation for the lateral friction of a pile foundation.

$$Q_s = u_c \sum q_{\text{sik}} l_i, \tag{7}$$

where u_c is the outer circumference of the lattice diaphragm wall, q_{sik} is the standard value of the ultimate lateral friction of the ith soil layer on the wall side, and l_i is the thickness of the ith soil layer on the wall side.

The wall end resistance, Q_p, is composed of the internal and external wall end resistance, Q_{pl}, and the diaphragm wall end resistance, Q_{pt}.

$$\begin{aligned} Q_p &= Q_{pl} + Q_{pt} \\ &= q_{pl} A_{pl} + q_{pt} A_{pt}, \end{aligned} \tag{8}$$

where A_{pl} is the section area of the internal and external walls, q_{plk} is the section area of the partition wall, q_{plk} is the allowable value of the bearing capacity of the soil at the end of the internal and external walls, and q_{ptk} is the allowable value of the bearing capacity of the soil at the end of the partition wall.

The lateral friction resistance, Q_{si}, of the core soil is given as follows:

$$Q_{si} = q_{st} A_{st}, \tag{9}$$

where q_{stk} is the allowable bearing capacity of the soil at the end of the wall core and A_{st} is the sectional area of the wall core.

Therefore, the equation for calculating the vertical bearing capacity of the lattice diaphragm wall in a loess area is shown in Figure 6.

$$\begin{aligned} Q_{uk} &= Q_{sk} - Q_{fk} + Q_{sik} - Q_{\text{fik}} + Q_{pk} \\ &= u_c \sum q_{\text{sik}} l_i + q_{\text{stk}} A_{st} + q_{\text{plk}} A_{pl} + q_{ptk} A_{pt} - Q_{fk} - Q_{\text{fik}}. \end{aligned} \tag{10}$$

4.2. Analysis of the Load-Settlement Law of a Single Lattice Diaphragm Wall in a Loess Area. The load transfer analysis method was proposed by Seed and Rees in 1957. It was first used to analyze the load transfer law of piles and to predict the settlement. This method divides the pile into several elastic elements along the pile body. Each element simulates the connection between the pile body and soil at the pile side as a grounded inelastic spring. The connection between the pile end and the soil has also been simulated as a nonlinear spring, as shown in Figure 7. The load transfer method was applied for analysis of the vertical bearing capacity of the diaphragm wall, and the load-settlement law of a single diaphragm wall was

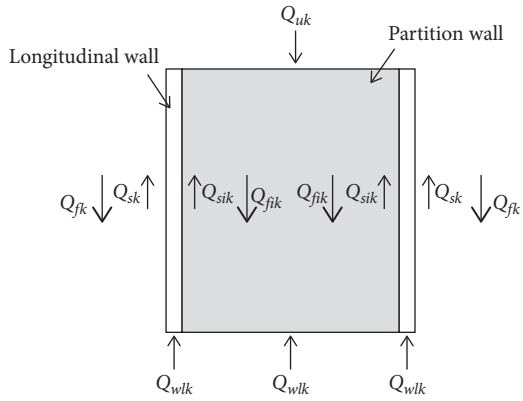

Figure 6: Diagram of the wall stress analysis.

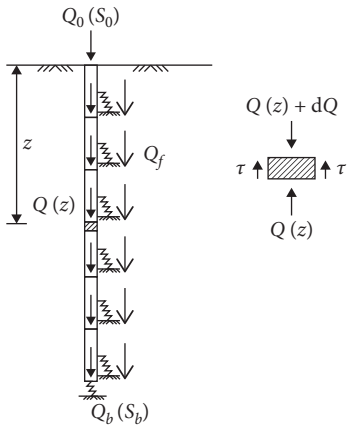

Figure 7: Diagram of the load transfer method.

analyzed. The vertical bearing capacity of the diaphragm wall could then be determined, and the vertical bearing characteristics of the diaphragm wall could be theoretically analyzed.

As shown in Figure 7, the analysis model of the diaphragm wall includes the load on the wall top and the settlement of the wall top. In this model, Q_p and S_p are the resistances at the end of the wall and the settlement at the end of the wall, respectively; $Q(z)$ and $\tau(z)$ are the load and side friction at the z section of the wall, respectively; and $\delta_s(z)$ and Q_f are the settlement and negative friction caused by the loess, respectively. Assuming that the diaphragm wall material is completely linearly elastic and will not be destroyed before reaching the ultimate bearing capacity, the load on the wall section at any depth z is as follows:

$$Q(z) = Q_0 - \int_0^{\tau} \tau_s(z)\mathrm{d}z + Q_f. \tag{11}$$

The vertical displacement of the wall section at any depth z is

$$S(z) = S_0 + \delta_s(z) - \frac{1}{EA}\int_0^{\tau} Q(z)\mathrm{d}z. \tag{12}$$

According to the equilibrium condition of the vertical force, the governing equation under a vertical load can be obtained from equation (5):

$$\begin{aligned}\tau(z) &= \frac{\mathrm{d}Q(z)}{\mathrm{d}z} + q \\ &= \frac{\mathrm{d}Q(z)}{\mathrm{d}z} - \frac{1}{U}EA\frac{\mathrm{d}^2u(z)}{\mathrm{d}^2z}.\end{aligned} \tag{13}$$

The compression, $\mathrm{d}S(z)$, of microelement $\mathrm{d}z$ is given as follows:

$$\mathrm{d}S(z) = -\frac{Q(z)}{EA}\mathrm{d}z. \tag{14}$$

The basic differential governing equation of the load transfer in the wall-soil system can be obtained as follows:

$$EA\frac{\mathrm{d}^2S(z)}{\mathrm{d}z^2} - \tau(z) = 0, \tag{15}$$

where E is the elastic modulus of the wall and A is the cross-sectional area of the wall.

It can be seen from equation (15) that the key to solving the fundamental equation for the load transfer of the wall-soil system is establishing a transfer function ($\tau(z) - S(z)$ function) that genuinely reflects the relationship between the lateral friction and shear displacement of the wall-soil interface. In a collapsible loess area, with increasing depth, the collapsible deformation of the soil causes relative displacement of the wall-soil interface and, consequently, negative friction on the wall side. As a result, the wall settlement increases, and the bearing capacity decreases. The wall displacement, $S(z)$, and wall load, $Q(z)$, show decreasing trends.

5. Discussion

5.1. Transfer Mechanism for the Side Friction Resistance of a Single Assembly Diaphragm Wall. For the ALDW, because of its high stiffness, the vertical load can be approximated as a rigid body, exhibiting a trend of overall subsidence. The side friction and end resistance of the diaphragm wall develop synchronously. Because the main bearing capacity of the diaphragm wall is wall side friction, the primary focus of the diaphragm wall load transfer mechanism is the mechanism of the wall side friction transmission.

Under a vertical load, the diaphragm wall and surrounding soil share the upper load through the shear action on the wall-soil interface. Under shear stress on the contact surface, relative displacement between the diaphragm wall and the soil occurs. Owing to the low stiffness of the soil itself, the shear stress on the contact surface leads to certain shear deformation of the soil around the wall. In general, shear deformation occurs around the wall without relative displacement between the wall and soil, which leads to a particular settlement of the diaphragm wall. With an increase in the vertical load on the wall top, the shear deformation of the soil around the wall further increases. The settlement of the ground wall increases, and the relative displacement between the diaphragm wall and soil around the wall increases gradually. When the vertical load reaches the ultimate load, the diaphragm wall will lose its stability. At

this time, the possible reasons for failure of the diaphragm wall are as follows: concrete failure of the diaphragm wall, shear failure of the soil around the wall, and failure of the diaphragm wall-soil interface.

The section size of the diaphragm wall is large, and the compressive rigidity of the concrete is usually also large. Therefore, the possibility of concrete failure is not significant. The main reasons for the failure of the diaphragm wall are described in the following.

5.1.1. Shear Failure of the Soil around the ALDW. If the shear strength of the diaphragm wall-soil interface is high and the mechanical properties of the soil around the wall are low, the failure of the ground wall is often caused by shear failure of the soil around the wall under a vertical load, as shown in Figure 8. When the vertical load is small, there is no relative displacement between the soil and the diaphragm wall along their interface, and the soil around the wall bears the shear load on the wall-soil interface. Because of the soil shear modulus, the diaphragm wall and soil on the wall side jointly bear the load applied on the wall top. The shear deformation of the soil causes settlement of the diaphragm wall. With an increase in the vertical load, the shear load of the soil around the wall increases, and the shear deformation also increases. When shear failure occurs in the soil around the wall owing to excessive shear deformation, the vertical load on the top of the diaphragm wall cannot be increased, which indicates that the diaphragm wall has been destroyed. At this time, it can be considered that the failure of the diaphragm wall is caused by shear failure of the soil around the wall, and the lateral friction of the diaphragm wall is determined by the mechanical properties of the soil around the wall.

The shear stress required for shear failure varies owing to the different stress states of the soil around the wall at different depths. As shown in Figure 9, the small circle indicates the stress state of the soil around a shallow wall in the equilibrium limit state, whereas the large circle indicates the stress state of the soil around a deep wall in the equilibrium limit state. Obviously, the greater the depth is, the higher the shear stress required for shear failure of the soil around the wall will be. Because the compression of the diaphragm wall is minimal, the settlement of the top of the wall is the same as the settlement of the wall, and thus it can be considered that the shear strain of the soil around the wall at different depths is the same. In other words, in the process of increasing the vertical load, the frictional resistance of the shallow wall first gives way and gradually develops to deeper areas.

5.1.2. ALDW-Soil Interface Damage. Under vertical loads, shear deformation of the soil around the wall may occur, and slipping may also occur between the diaphragm wall and the soil around the wall. When the shear strength of the interface is not greater than the shear strength of the soil around the wall, sliding failure of the interface between the diaphragm wall and the soil usually precedes shear failure of the soil around the wall. At this time, the vertical bearing capacity of the diaphragm wall mainly depends on the mechanical properties of the interface between the wall and the soil, and the limit value of the wall side friction resistance has a greater effect than that of the wall-soil interface.

During construction of the diaphragm wall, mud is typically used to protect the wall. If the mud is thick, the shear strength of the wall-soil interface can easily be reduced. In addition, during excavation of diaphragm wall trenching, the mechanical properties of the soil around the wall in a certain range decrease to a greater extent due to the construction disturbance, and the shear strength of the wall-soil interface may also be reduced. In these two cases, the inducement of the failure at the wall-soil interface is different, but the failure mechanisms are similar. When the load on the wall top reaches a certain level, relative slip occurs between the ground wall and the soil around the wall, and the sliding surface is in a vertical state, as shown in Figure 10. With an increase in the vertical load, the relative displacement between the diaphragm wall and soil around the wall increases, but the development of shear deformation around the wall is not apparent. When the wall-soil interface is destroyed due to excessive relative displacement, the load on the top of the wall cannot continue to increase, and the wall is destroyed by instability. At this time, it can be considered that failure of the wall-soil interface causes the failure of the diaphragm wall, and the lateral friction of the diaphragm wall is determined by the mechanical index of the wall-soil interface.

In the process of vertical loading on the wall top, soil shear deformation around the wall occurs, and the shear stress at the interface of the wall and the soil around the wall is balanced. Because the diaphragm wall sinks as a whole, the shear strain of the soil around the wall is the same, and thus the shear stress along the wall depth is the same at all parts of the wall-soil interface. With an increase in the load on the wall top, the shear stress on the contact surface between the wall and soil at the shallow part of the wall reaches the shear strength of the contact surface first, and relative slip along the contact surface occurs between the shallow part of the diaphragm wall and the soil around the wall. When the load on the top of the wall increases further, the shear strain of the soil around the shallow wall ceases to increase because the shear strength of the interface of the shallow wall and the shear strain of the deep soil continue to increase until the shear stress on the interface between the deep wall and soil reaches the shear strength of the interface. Therefore, it can be considered that if the top wall load is increasing, the cause of wall instability is sliding failure of the wall-soil interface, and the development process is from the top of the wall to the bottom of the wall.

If the foundation soil around the diaphragm wall is not improved or reinforced, the surface of the diaphragm wall is sufficiently rough, and the shear strength of the interface between the wall and the soil is sufficiently large, shear failure of the foundation soil around the wall is the leading cause of the instability failure of the diaphragm wall in the process of increasing the load on the top of the wall.

In this case, the limit value of the wall side friction is determined by the mechanical index of the foundation soil. In construction of the diaphragm wall, a certain thickness of mud interlayer is formed between the wall and soil because

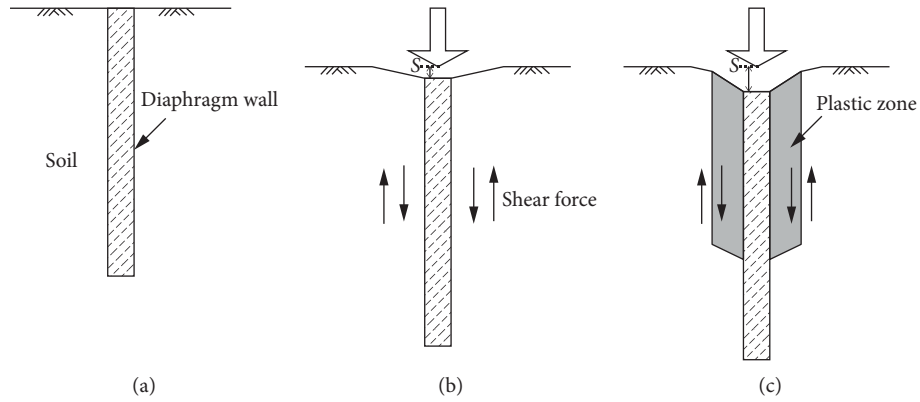

Figure 8: Shear failure of the soil around the wall.

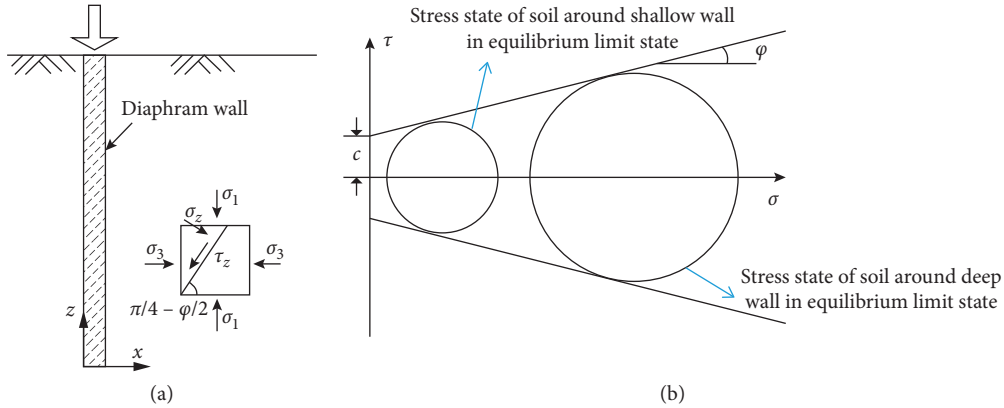

Figure 9: Stress state of the soil around the wall. (a) Stress strains of the soil around the wall. (b) Shear strain of the soil around the wall at different depths.

of the thick mud skin, or the strength of the soil around the wall is reduced; as a result, the shear strength of the interface between the diaphragm wall and soil becomes weak due to construction disturbance. Therefore, shear failure of the interface occurs before shear failure of the soil around the wall. In this case, as the load increases on the wall top, shear failure of the interface between the wall and soil causes instability failure of the ground wall. The ultimate value of the wall frictional resistance is determined by the mechanical index of the wall-soil interface. The ultimate value of the wall frictional resistance is smaller than that of the pile-side frictional resistance when the shear failure mode occurs in the soil around the pile.

5.2. Factor Analysis of the Vertical Bearing Behavior of a Lattice Diaphragm Wall in a Loess Area. Many factors affect the vertical bearing behavior of a lattice diaphragm wall in a loess area, including (1) the elastic modulus, $E1$, and Poisson's ratio, $\mu 1$, at the side of the wall; (2) the elastic modulus, $E2$, and Poisson's ratio, $\mu 2$, at the end of the wall; (3) the cohesion, $c1$, and internal friction angle, $\varphi 1$; (4) the cohesion, $c2$, and internal friction angle, $\varphi 2$, at the end of the wall; (5) the static lateral pressure coefficient of the soil, $K0$; (6) the friction coefficient of the wall-soil interface, μ, and the allowable relative sliding, r; (6) the degree of immersion; (7) the collapsibility grade and stress history of the soil layer around the wall; and (8) the length-to-diameter ratio of the wall and other factors.

5.3. Analysis of Influence of Excavation Process on Stress of ALDW. Based on ABAQUS, a three-dimensional finite element model of multigrid diaphragm wall is established to analyze the deformation and stress characteristics with different excavation depth. The simulated excavation depth of the foundation pit is 15 m, the depth of the lattice diaphragm wall is 30 m, the thickness of the wall is 0.8 m, the spacing between the horizontal partition wall axis is 6.0 m, and the spacing between the front and rear walls is 8.0 m. The size of the whole model is 103 m × 60 m × 30 m (Figure 11). Considering the influence of the construction steps on the foundation pit supporting structure, the excavation steps are divided into three steps when modeling; the excavation depth of each step is 5 m.

The Mohr-Coulomb ideal elastic-plastic model is adopted for soil constitutive model, in which the soil is divided into three layers for calculation, and the calculation parameters of each layer are shown in Table 1. The diaphragm wall is made of C35 concrete with elastic modulus of 35.1 GPa, Poisson's ratio of 0.2, and density of

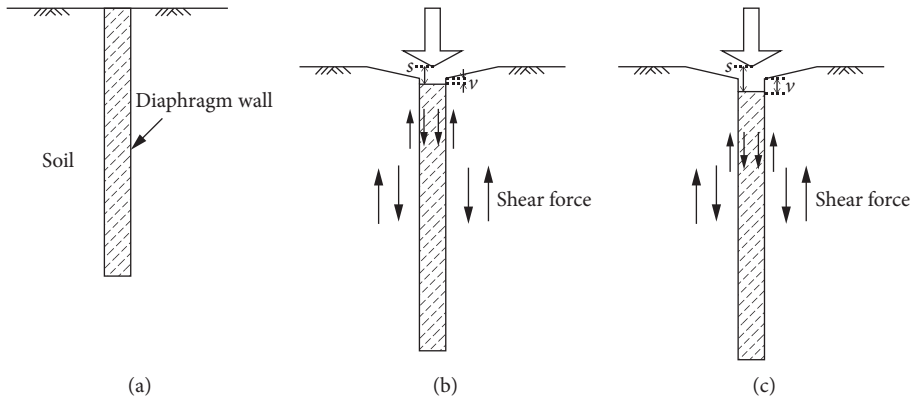

Figure 10: Shear failure of the wall-soil interface.

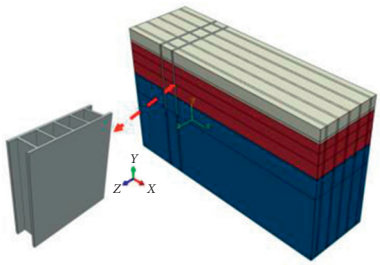

Figure 11: Numerical calculation model of ALDW.

2500 kg/m^3. The influence of groundwater is not considered in the analysis. The following assumptions are made in the simulation:

(1) The drainage consolidation of soil is not considered

(2) Soil excavation is completed instantaneously without considering time effect

If the position of the front and rear walls is shown in Figure 12, the internal force distribution nephogram of the step-by-step excavation lattice diaphragm wall (Figure 13) and the shear stress distribution curve of the front and rear walls and diaphragm wall (Figure 14) are obtained by numerical calculation. The positive value in the figure represents the tensile stress of the wall, and the negative value represents the compressive stress of the wall. It can be seen from Figure 13 that the internal force of diaphragm wall is larger at the bottom than at the top of the wall, the embedded section is larger than the excavation section, and the stress of the front wall > the stress of the cross wall > the stress of the back wall. The maximum stress appears at the bottom of the front wall, which is lower than the compressive limit of concrete. The stress at the top of the wall is far less than that at the bottom of the wall, and the stress concentration appears at the end of the front wall. After the excavation of foundation pit, the front and rear walls move to the pit under the action of unbalanced Earth pressure, and the soil in the pit prevents the wall from moving laterally, so the pressure on the embedded section of the front wall is greater.

It can be seen from Figure 14 that the shear stress of the front wall increases linearly along the depth direction of the wall, and the wall is compressed. The shear stress of the back wall and the transverse wall changes nonlinearly along the depth direction of the wall. The cantilever section is compressed and the embedded section is tensioned along the depth direction of the wall. The cantilever section of the transverse partition wall is in tension along the depth direction of the wall, while the embedded section is in compression. With the increase of excavation depth, the shear stress of the front wall increases, and the maximum shear stress is 1.56 mpa. In the consolidation stage, the compressive stress of the back wall increases linearly along the depth of the wall. With the increase of excavation depth, the shear stress of back wall presents "*s*" type distribution, the compressive stress of cantilever section increases, and the compressive stress of embedded section decreases. When the excavation is 15 m, the tensile stress appears at the depth of 20 m. This is due to the excavation of the foundation pit; there is an unbalanced Earth pressure inside and outside the wall, which makes the wall move to the inside of the foundation pit. The pressure of the front wall is greater than that of the back wall, which prevents the wall from lateral displacement. At the same time, the tensile stress of the upper part of the transverse partition also prevents the wall from lateral displacement, so the tensile stress appears in the wall of the embedded section. It can be seen from Figure 14(c) that the stress of the transverse partition wall changes in an inverse "*s*" curve. Along the depth direction of the wall, the cantilever section is in tension and the embedded section is in compression. With the increase of excavation depth, the tensile stress of the wall increases and the compressive stress decreases. The stress of the wall changes from tension to compression, because the wall is cantilever structure, which dumps to the excavation side under the back pressure. The cross wall connects the front wall and the back wall and prevents the wall from moving to the foundation pit under the back wall gravity stress and the soil on both sides of the cross wall. When the back wall Earth pressure is greater than the wall side friction, the wall moves to the inside of the foundation pit, and the cross wall is compressed. The greater the excavation depth, the greater the tensile stress and the smaller the compressive stress. The results show that the function of transverse wall and back wall is the main reason why the fabricated lattice diaphragm wall can be used for foundation pit excavation without internal support structure.

Table 1: Soil layer calculation parameter.

Soil layer number	Thickness h (m)	Soil weight γ (kN/m^3)	Cohesion c (kPa)	Internal friction angle φ (°)	Elastic modulus E (kPa)	Poisson's ratio ν
1	6	19.4	25	18	25000	0.31
2	15	20	35	19	33000	0.35
3	39	19.3	48	22	80000	0.35

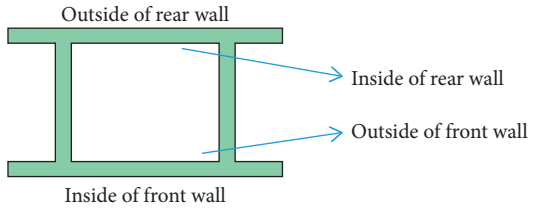

Figure 12: Location of front and back walls of lattice diaphragm wall.

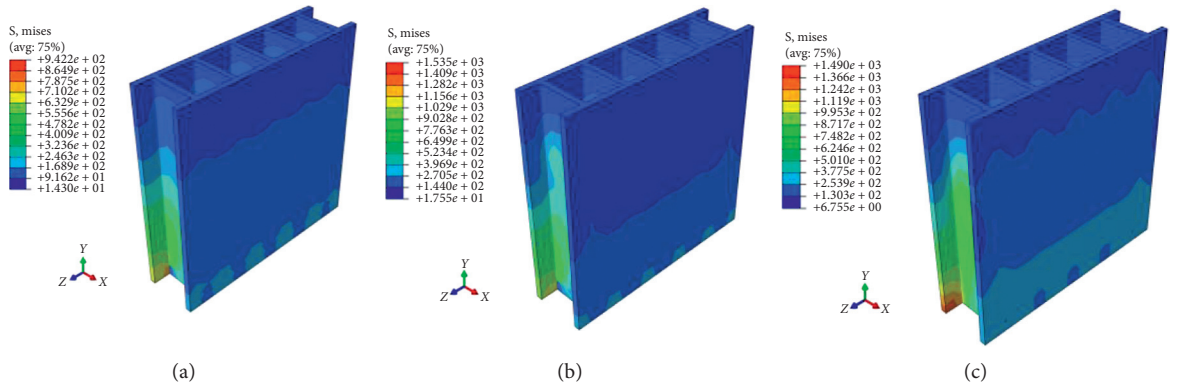

(a) (b) (c)

Figure 13: Internal force distribution of ALDW excavation. (a) Excavation of the first layer. (b) Excavation of the second layer. (c) Excavation of the third layer.

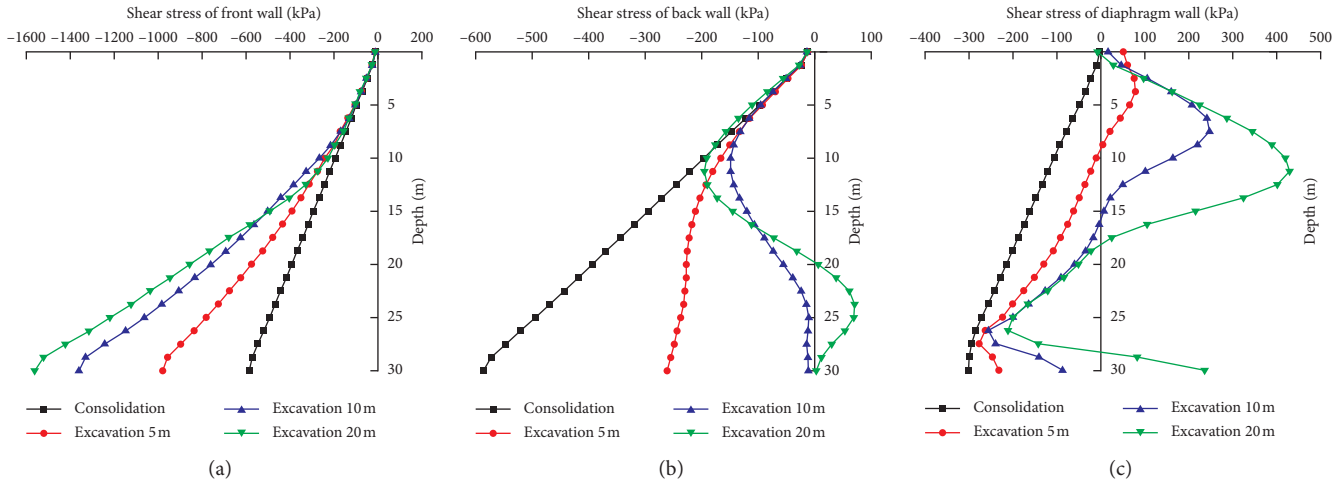

(a) (b) (c)

Figure 14: Shear stress distribution curve of ALDW. (a) Shear stress of front wall. (b) Shear stress of back wall. (c) Shear stress of diaphragm wall.

6. Conclusions

The load transfer method was used to analyze the process of negative friction and the transfer of collapsible displacement of an ALDW in a collapsible loess area. A preliminary theoretical analysis of the vertical bearing mechanism was carried out for the ALDW in a collapsible loess area. The main conclusions are as follows:

(1) The collapse process is formally expressed as the conversion of physical force (gravity) to surface force (negative friction). The closer the collapse is to the wall, the more energy is dissipated through plastic deformation and the smaller the shear deformation will be under the same shear stress. The negative friction, q, is distributed irregularly along the wall. The relative displacement between the wall and soil at the neutral point is zero; at this point, the friction resistance is zero, and the axial force is the maximum. The neutral position also varies with time.

(2) The equation for calculating the vertical bearing capacity of a lattice diaphragm wall in a loess area was deduced, and the load-settlement law for a single lattice diaphragm wall in a loess area was analyzed. In the collapsible loess area, with an increase in depth, the collapsible deformation of the soil causes relative displacement between the wall and soil, resulting in negative friction resistance on the wall side and leading to wall settlement. As the depth increases, the load-bearing capacity decreases.

(3) By analyzing the transfer mechanism of side friction of single assembled diaphragm wall, it is concluded that the main failure types are shear failure of soil around ALDW and failure of interface between continuous wall and soil.

(4) The factors affecting vertical bearing capacity of ALDW in loess area mainly include the mechanical properties of soil at side and end of wall, collapsibility grade of soil around wall, the degree of immersion and stress history, and the length-diameter ratio of the wall.

Data Availability

The data used to support the findings of this study are included within the article.

Conflicts of Interest

The authors declare that they have no conflicts of interest.

Acknowledgments

This work was supported by the National Key R&D Program of China (Grants No. 2018YFC0808705), National Natural Science Foundation of China (Grants No. 41702339), and the project supported by Natural Science Basic Research Plan in Shaanxi Province of China (Grants No. 2018JQ4026).

References

[1] J.-j. Wu, Q.-g. Cheng, H. Wen, and J.-l. Cao, "Comparison on the vertical behavior of lattice shaped diaphragm wall and pile group under similar material quantity in soft soil," *KSCE Journal of Civil Engineering*, vol. 19, no. 7, pp. 2051–2060, 2015.

[2] Q. Cheng, J. Wu, Z. Song, and H. Wen, "The behavior of a rectangular closed diaphragm wall when used as a bridge foundation," *Frontiers of Structural and Civil Engineering*, vol. 6, no. 4, pp. 398–420, 2012.

[3] Y. Arai, O. Kusakabe, O. Murata, and S. Konishi, "A numerical study on ground displacement and stress during and after the installation of deep circular diaphragm walls and soil excavation," *Computers and Geotechnics*, vol. 35, no. 5, pp. 791–807, 2008.

[4] C. De Lyra Nogueira, R. F. De Azevedo, and J. G. Zornberg, "Coupled analyses of excavations in saturated soil," *International Journal of Geomechanics*, vol. 9, no. 2, pp. 73–81, 2009.

[5] R. Schäfer and T. Triantafyllidis, "Modelling of earth and water pressure development during diaphragm wall construction in soft clay," *International Journal for Numerical and Analytical Methods in Geomechanics*, vol. 28, no. 13, pp. 1305–1326, 2004.

[6] C. Yoo and D. Lee, "Deep excavation-induced ground surface movement characteristics—a numerical investigation," *Computers and Geotechnics*, vol. 35, no. 2, pp. 231–252, 2008.

[7] Y. Chen, H. Lin, Y. Wang, R. Cao, C. Zhang, and Y. Zhao, "Modified double-reduction method considering strain softening and equivalent influence angle," *KSCE Journal of Civil Engineering*, vol. 24, pp. 1–10, 2020.

[8] Y. Mei, "Measured deformation of self-supporting lattice concrete diaphragm walls," *Chinese Journal of Geotechnical Engineering*, vol. 32, no. S1, pp. 463–467, 2010.

[9] S. Liang, W. Xu, and Y. Chen, "Lateral deformation of cellular diaphragm wall at excavation stage," *Journal of Southwest Jiaotong University*, vol. 50, no. 1, pp. 150–155, 2015.

[10] Y. Zuo, W. Xu, and Z. Xu, "Centrifugal model tests on mechanical property of gridding continuous diaphragm walls in sand," *Chinese Journal of Geotechnical Engineering*, vol. 32, no. S1, pp. 473–477, 2010.

[11] G. Zhou, W. Xu, and Y. Chen, "Centrifugal model test study of interaction of gridding concrete retaining wall and soft soil," *Rock and Soil Mechanics*, vol. 32, no. S1, pp. 134–140, 2011.

[12] X. Chen, W. Xu, and Y. Zuo, "Centrifugal model tests on mechanical property of cellular diaphragm wall," *Industrial Construction*, vol. 43, no. 2, p. 67, 2013.

[13] Y. Hou, *Behavior of cellular diaphragm wall in soft deposit*, Ph.D. thesis, Shanghai Jiao Tong University, Shanghai, China, 2010.

[14] T. Masuda, *Behavior of Deep Excavation with Diaphragm Wall*, Massachusetts Institute of Technology (MIT), Cambridge, MA, USA, 1993.

[15] D. R. Carder, *Ground Movements Caused by Different Embedded Retaining Wall Construction Techniques*, Vol. 172, Transport Research Laboratory Report, Berkshire, UK, 1995.

[16] C. Yoo, "Behavior of braced and anchored walls in soils overlying rock," *Journal of Geotechnical and Geoenvironmental Engineering*, vol. 127, no. 3, pp. 225–233, 2001.

[17] C. Moormann, "Analysis of wall and ground movements due to deep excavations in soft soil based on a new worldwide database," *Soils and Foundations*, vol. 44, no. 1, pp. 87–98, 2004.

[18] M. Long, "Database for retaining wall and ground movements due to deep excavations," *Journal of Geotechnical and Geoenvironmental Engineering*, vol. 127, no. 33, pp. 203–224, 2001.

[19] J.-j. Wu, L.-j. Wang, and Q.-g. Cheng, "Soil arching effect of lattice-shaped diaphragm wall as bridge foundation," *Frontiers of Structural and Civil Engineering*, vol. 11, no. 4, pp. 446–454, 2017.

[20] J. Wu, Q. Cheng, H. Wen, and J. L. Cao, "Vertical bearing behaviors of lattice shaped diaphragm walls and group piles as bridge foundations in soft soils," *Chinese Journal of Geotechnical Engineering*, vol. 36, no. 9, pp. 1733–1744, 2014.

[21] L. I. Tao, "Research on the calculation of diaphragm wall as bridge foundation in loess," *Chinese Journal of Geotechnical Engineering*, vol. 19, no. 3, pp. 47–54, 1997.

[22] G. Dai, W. Gong, X. Zhou, Y. Liu, and L. Liu, "Experiment and analysis on horizontal bearing capacity of single-chamber closed diaphragm wall," *Journal of Building Structures*, vol. 33, no. 9, pp. 67–73, 2012.

[23] Q. Cheng, "Mechanism of LSDW as bridge foundation against seismic liquefaction," *Academic News*, vol. 41, no. 1, pp. 35–44, 2014.

[24] Y.-m. Hou, *Behavior of Cellular Diaphragm wall in Soft Soil*, Shanghai Jiao Tong University, Shanghai, China, 2010.

[25] Y.-m. Hou, "Vertical bearing behaviors of cellular diaphragm wall," *Chinese Journal of Geotechnical Engineering*, vol. 34, no. 4, pp. 701–708, 2012.

[26] M. Xie, J. Zheng, J. Dong, and C. Miao, "Foundation improvement with lattice-shaped diaphragm wall treatment for high embankment culverts on soft foundation," *Tunnelling and Underground Space Technology*, vol. 10, no. 104, Article ID 103535, 2020.

[27] J. J. Wu, Q. G. Cheng, H. Wen, Y. Li, J. L. Zhang, and L. J. Wang, "Comparison on the horizontal behaviors of lattice-shaped diaphragm wall and pile group under static and seismic loads," *Shock and Vibration*, vol. 2016, Article ID 1289375, 17 pages, 2016.